OPEN

Diagnostic Value of Contrast-Enhanced Spectral Mammography in Comparison to Magnetic Resonance Imaging in Breast Lesions

Dong Xing, BS, Yongbin Lv, MSc,* Bolin Sun, MSc,† Haizhu Xie, MSc,* Jianjun Dong, MSc,* Cuijuan Hao, BS,* Qianqian Chen, PhD,‡ and Xiaoxiao Chi, MSc**

Objective: The aim of this study was to evaluate the diagnostic value between contrast-enhanced spectral mammography (CESM) and breast magnetic resonance imaging (MRI) in breast disease.

Methods: Two hundred thirty-five patients who were suspected of having breast abnormalities by clinical examination or mammography underwent CESM and MRI examination. Using histopathologic results as the criterion standard, the diagnostic performance of CESM and MRI was investigated. The areas under receiver operating characteristic curves were applied to analyze diagnostic efficiency. The Pearson correlation coefficients between CESM versus pathology and MRI versus pathology were calculated.

Results: Two hundred sixty-three breast lesions were found in 235 patients, in which 177 were malignant and 86 were benign. By evaluating the diagnostic value, sensitivity, positive predictive value, negative predictive value, and false-negative rate from CESM examination were comparable to those from MRI (91.5%, 94.7%, 83.7%, and 8.5% vs 91.5%, 90.5%, 82.1%, and 8.5%). Importantly, the accuracy and the specificity were higher for CESM than those for MRI (81% and 89.5% vs 80.2% and 71.7%), whereas the false-positive rate was lower (10.5% vs 19.8%). The areas under receiver operating characteristic curves of CESM and MRI were 0.950 and 0.939, displaying the equivalent diagnostic efficiency ($P = 0.48$). For the agreement between measurements, mean tumor sizes were 3.1 cm for CESM and 3.4 cm for MRI compared with 3.2 cm on histopathologic results. The Pearson correlation coefficient of CESM versus histopathology ($r = 0.774$, $P = 0.000$) was consistent with MRI versus histopathology ($r = 0.771$, $P = 0.000$).

Conclusions: Our results show better accuracy, specificity, and false-positive rate of CESM in breast cancer detection than MRI. Contrast-enhanced spectral mammography displayed a good correlation with histopathology in assessing the lesion size of breast cancer, which is consistent with MRI.

Key Words: breast cancer, contrast agent, contrast-enhanced spectral mammography, magnetic resonance imaging

(*J Comput Assist Tomogr* 2019;43: 245–251)

From the *Department of Radiology and †Interventional Therapy Ward, Yantai Yuhuangding Hospital; and ‡The Affiliated Yantai Yuhuangding Hospital of Qingdao University, Yantai, China.

Received for publication May 30, 2018; accepted October 9, 2018.

Correspondence to: Xiaoxiao Chi, Department of Radiology, Yantai Yuhuangding Hospital, No. 20, Yuhuangding East Road, Yantai, Shandong Province 264000 China(e-mail: chixiaoxiao87@126.com).

D.X., Y.L., and B.S. contributed equally to this work.

D.X., Y.L. and B.S. are co- first authors.

The authors declare no conflict of interest.

DOI: 10.1097/RCT.0000000000000832

Contrast-enhanced spectral mammography (CESM) is a novel imaging technique using a dual-energy technique to detect breast cancer. It is based on the contrast enrichment due to newly formed proliferating tumor vessels and the high permeability within tumor regions. Contrast-enhanced spectral mammography is performed with high-energy (HE) and low-energy (LE) acquisitions after the injection of iodine contrast medium, so as to obtain the recombined images of bilateral breasts. The LE image presents the morphological information equivalent to 2-dimensional (2D) digital mammography, whereas the HE image displays the post–contrast-enhanced mammograms by utilizing the K-edge effect of iodine, to evaluate tumor neovascularity.[1] Given these benefits, CESM has been proven to be a viable alternative imaging tool in the detection of breast cancer.[2] Previous reports have shown that, as compared with traditional 2D mammography, application of CESM significantly increased positive rate, accuracy, and sensitivity for breast cancer detection and reduced the mortality of breast cancer because this recombined image could overcome the overlapping of normal breast tissues and eliminate the fibrous glands of breasts.[3,4] Additionally, CESM displays a decrease in the false-positive rate, high specificity, and an improvement in size estimation, suggesting a significance impacting on downgrading mammographic lesions[4–6] and reducing the recall rates.[1,7]

Breast magnetic resonance imaging (MRI) is the most accurate imaging tool in diagnosing breast cancer because of high sensitivity to soft tissues. At present, breast MRI can provide more comprehensive diagnostic information to identify the benign and malignant breast lesions that are not definitely diagnosed by mammography and ultrasonography. The current studies have confirmed that the sensitivity of MRI is up to 80% to 97.8%, but the specificity is only 46% to 93.3% in diagnosing breast cancer, leading to high rates of misdiagnosis.[8] Additional study with information on MRI and breast cancer surgical performance indicated 5.5% conversion to extensive surgery for false-positive MRI examination.[9] The application of CESM may be alternative for diagnosing breast cancer. Besides that, access to MRI is limited to large space, the procedure is expensive and time consuming, and it is contraindicated in patients with metallic implants and pacemaker. Contrast-enhanced spectral mammography is faster and easier to implement into practice and much cheaper than MRI.[1,2]

Contrast-enhanced spectral mammography is in its early stages of development and clinical use. This work was aimed to explore the diagnosis efficiency of CESM, by comparing with MRI and pathological results. We calculated some indicators, including sensitivity, specificity, and so on, to discuss the feasibility study of CESM in diagnosing breast diseases.

MATERIALS AND METHODS

Study Population

This work approved by the ethics committee of Yantai Yuhuangding Hospital, and all subjects provided the informed consent before examination. The study duration was 8 months starting from July 2017 to January 2018. All patients enrolled in this study were selected based on the following criteria: (1) patients suspected with abnormal breast lesions by the clinical examination or ultrasonography, (2) patients whose breast structure could be completely visualized in the CESM digital display screen, (3) patients who could undergo the breast CESM and MRI examinations within 1 week, and (4) patients whose final diagnosis was confirmed by pathology. The exclusion criteria were described below: (1) women who were pregnant, planned to get pregnant, or were lactating; (2) patients with severe diseases who were unable to cooperate in the examination; (3) patients with a history of breast surgery within 5 years; (4) patients known or suspected to be sensitive to iodine contrast media or other contrast media; and (5) patients known to have or suspected of having renal insufficiency. Eventually, 235 patients were included into the study, and all of them were female and aged 51 ± 10 years (range, 25–82 years).

Imaging examination techniques

Contrast-Enhanced Spectral Mammography

All the CESM examinations were performed using GE Senographe Essential mammography unit (GE Healthcare, Milwaukee, WI). The CESM imaging protocol was described in detail previously.[1] Briefly, a pair of images, consisting of a HE image (45–49 kVp) and a LE image (26–32 kVp), was obtained consecutively. The contrast medium (iohexol) at 1.5 mL/kg body weight (containing 300–350 mg/mL iodine) and a rate of 3 mL/s was administrated using a power injector. Two minutes after injection, a typical 4-view examination was carried out in the sequence of the craniocaudal position of abnormal breast → the craniocaudal position of abnormal breast → the medial-lateral oblique position of normal breast → the medial-lateral oblique position of normal breast, and the photography of 4-view examination for each patient was finished within 7 minutes. During photography at the projection positions, a recombined image was successively obtained within 1.5 seconds during a single compression. All these images were generated using a fully automatic, locally adjusted, tissue thickness–dependence process.

Magnetic Resonance Imaging

The MRI examinations were carried out on GE Signa HDXT 3.0-T whole-body MR scanner system (GE Healthcare, Milwaukee, WI). The patients were in a supine position with bilateral breasts loosing naturally within the breast-dedicated coils. The contrast medium (Gd-DTPA) was used and injected at 2 mL/s rate by a dose of 0.2 mmol/kg. The plain scan sequences of MR scanner included: T1-weighted imaging, scan parameters: repetition time (TR) = 750.0 milliseconds, time to echo (TE) = 10.0 milliseconds, number of excitations (NEX) = 1; axial fast relaxation fast spin echo T2-weighted imaging, scan parameters: TR = 4000.0 milliseconds, TE = 38 milliseconds, NEX = 2. Other parameters were as follows: slice thickness: 5.0 mm, interval-free scan, matrix = 384 × 192, and field of view = 360 × 360 mm. For dynamic enhanced scanning, the cross-sectional breast dynamic volume imaging sequence was used, and the scan parameters were as follows: TR = 4.0 milliseconds, TE = 2.0 milliseconds, slice thickness: 1.5 mm, interval-free scan, matrix = 320 × 256, field of view = 320 × 320 mm, NEX = 1. Eight phases were successively acquired without interval before and after contrast medium injection, the single scan time was 60 seconds, and the number of single-phase scan slices was 64.

Analysis of CESM Images

After the completion of acquisition, all images were automatically sent to a picture archiving and communication system system. The images obtained with 2 imaging techniques were diagnosed in a double-blind method by 3 radiologists with 10-year working experience in breast imaging. These radiologists assessed the lesions independently by Breast Imaging Reporting and Data System (BI-RADS) grading and measured the maximum diameter of suspected lesions. For the cases with different scores made by the 3 radiologists, a final score would be provided after negotiation. The breast lesions were evaluated according to the standards in the breast imaging report and data system (2013). For CESM imaging reading, in addition to BI-RADS classification of LE imaging similar to 2D digital mammography, the HE imaging reading standard was added according to MRI standard, including the presence of enhancement in the subtraction images and the morphological characteristics of enhanced lesions.[10] The CESM imaging interpretation of breast lesions was based on the following criteria: (1) having an irregular morphology and being markedly enhanced in the subtraction image, the lesion was assessed as malignant (Fig. 1); (2) being nonenhanced or having a regular morphology and being mildly enhanced in the subtraction image, the lesion was assessed as benign (Fig. 2). For the diagnostic feature of lesions, the lesion at BI-RADS 4A and below was diagnosed as benign, and that at BI-RADS 4B and above was diagnosed as malignant. For the detection of lesions, BI-RADS 0 and 1 indicated no lesion, and BI-RADS 2 or greater indicated a lesion. With the pathological results as criterion standard, the diagnostic efficacy was compared among different images.

Pathological Evaluation of Specimens

All specimens were fixed, embedded and sectioned, and then subjected to conventional hematoxylin-eosin (HE) staining and immunohistochemical analysis. All pathological sections were evaluated by 2 pathologists referring to World Health Organization Pathological Classification and Diagnostic Criteria of Breast Tumors (2012) to obtain their pathological results. The maximum diameter of lesions was measured. We used a ruler to assess the gross specimen for large specimens, whereas the small specimens were measured under a microscope. For the cases with different scores made by the 3 radiologists, a final score would be provided after negotiation.

Statistical Analysis

All measurement results are the means of the results obtained by 3 observers. The interobserver agreement was analyzed with κ test: $0 < \kappa \leq 0.4$ suggested bad agreement, $0.4 < \kappa < 0.75$ suggested good agreement, and $0.75 \leq \kappa < 1$ suggested excellent agreement.

The measurement data were presented as mean ± SD ($x \pm s$). With the pathological results as criterion standard, the capabilities of CESM and MRI to predict breast disease were evaluated by receiver operating characteristic (ROC) curve analysis. The area under curve (AUC) was compared with z test, and $P < 0.05$ suggests that a difference was statistically significant. The cutoff was determined according to ROC curve, and then the specificity and sensitivity of various scoring systems were calculated separately. The correlation between the maximum diameters of lesions measured by CESM and MRI and by pathology was investigated by Pearson nonparameter correlation analysis.

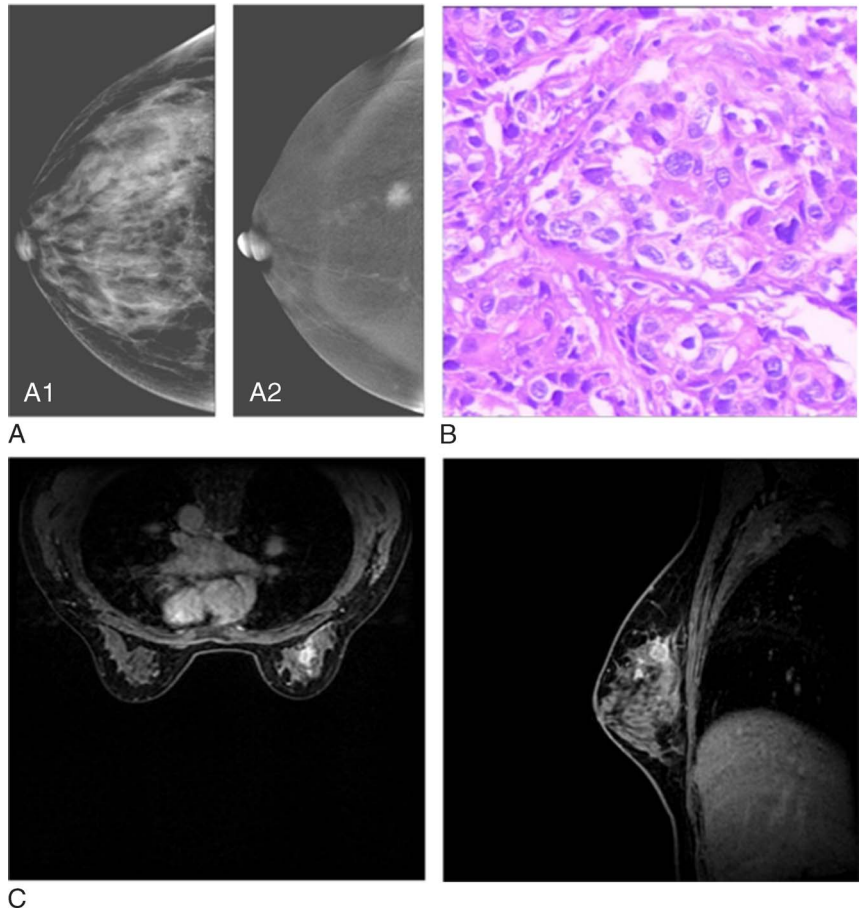

FIGURE 1. In CESM imaging, the LE (A1) image shows a diffuse high-density shadow in the right breast, with an unclear border and irregular edges; the subtraction image (A2) shows the significantly nonuniform enhancement of lesions in the outer quadrant of left breast. It is confirmed by pathological results as infiltrative ductal carcinoma (B). Magnetic resonance imaging scan shows a similar lump-like enhancement(C). Figure 1 can be viewed online in color at www.jcat.org.

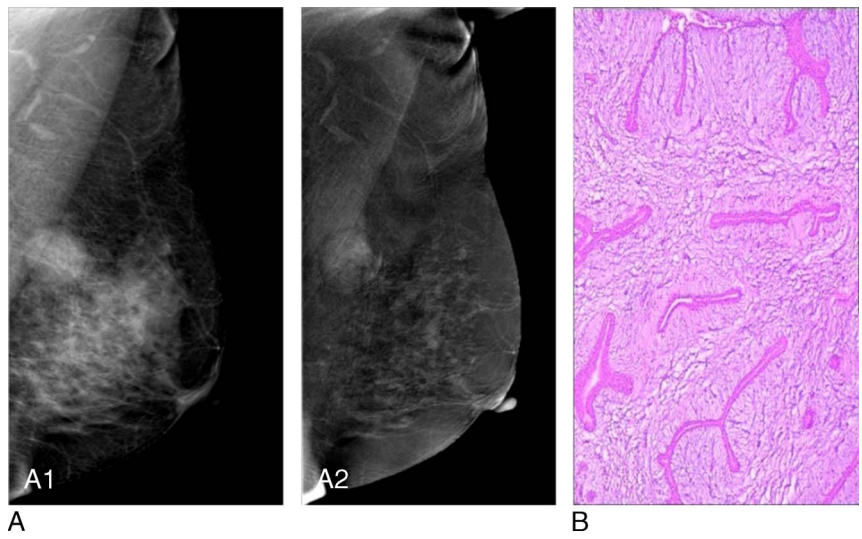

FIGURE 2. In CESM imaging, the LE image (A1) shows an oval lump shadow in the upper quadrant of left breast, with a clear border and regular edges; the subtraction image (A2) shows mild enhancement of lesions in the upper quadrant of left breast, with an obvious border. It is confirmed by pathological results as fibroadenoma (B). Figure 2 can be viewed online in color at www.jcat.org.

TABLE 1. The Pathological Diagnosis of Breast Lesions

Benign Lesions	n	Malignant Lesions	n
Fibroadenoma	26	Infiltrative ductal carcinoma	117
Adenosis	15	Ductal carcinoma in situ	6
Fibroadenoma with adenosis	9	Infiltrative ductal carcinoma with ductal carcinoma in situ	43
Intraductal papilloma	14	Infiltrative lobular carcinoma	1
Cystic adenosis	12	Papillary carcinoma	4
Chronic inflammation	2	Mucinous adenocarcinoma	3
Benign lesions	8	Colloid carcinoma	1
		Infiltrative ductal carcinoma with apocrine carcinoma	2

The measurement data were analyzed on SPSS 13.0 statistical software (Chicago, IL), whereas AUC was computed on MedCalc statistical software (Ostend, Belgium). $P < 0.05$ suggested that a difference was statistically significant.

RESULTS

Pathological Diagnosis

In 235 patients, in total 263 lesions were detected, including bilateral lesions in 20 cases, unilateral breast lesion in 209 cases, and 2 unilateral breast lesions in 8 cases. There were 86 benign lesions (including 26 lesions of fibroadenoma, 15 lesions of adenosis, 9 lesions of fibroadenoma with adenosis, 14 lesions of intraductal papilloma, 12 lesions of cystic adenosis, 8 benign lesions, and 2 lesions of chronic inflammation) and 177 malignant lesions (including 117 lesions of infiltrative ductal carcinoma, 6 lesions of ductal carcinoma in situ, 43 lesions of infiltrative ductal carcinoma with ductal carcinoma in situ, 1 lesion of infiltrative lobular carcinoma, 4 lesions of papillary carcinoma, 3 lesions of mucinous adenocarcinoma, 1 lesion of colloid carcinoma, and 2 lesions of infiltrative ductal carcinoma with apocrine carcinoma) (Table 1).

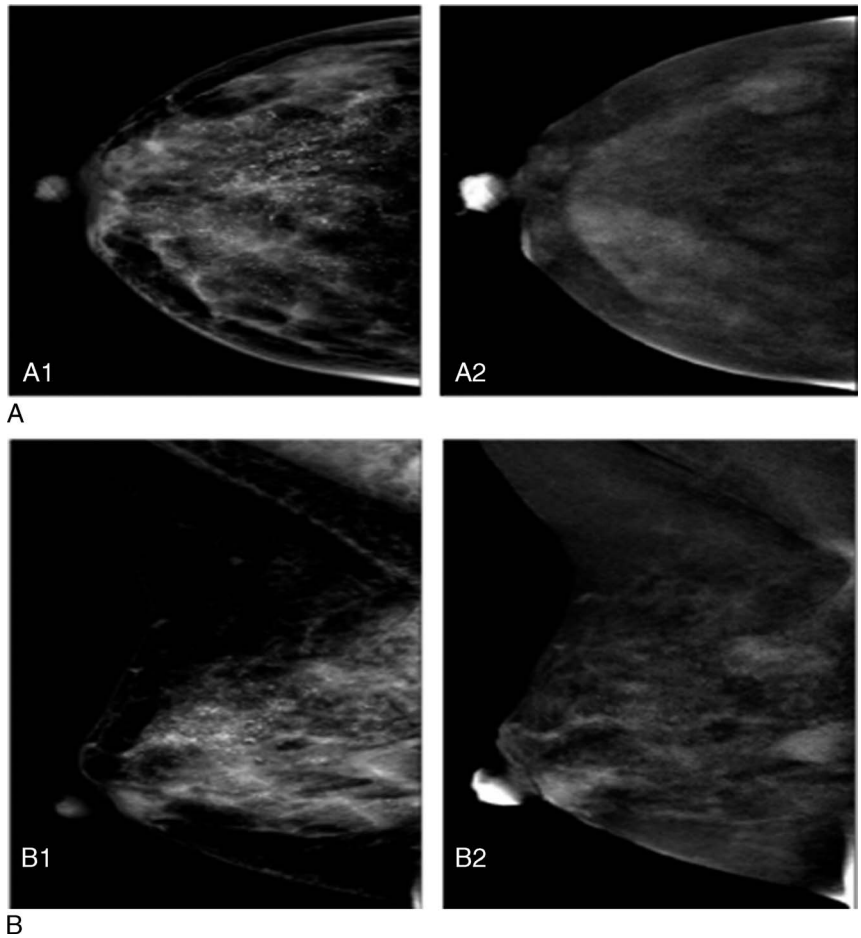

FIGURE 3. In CESM imaging, the LE image (A1, B1) shows gravel-like unshaped calcifications diffusely distributed in the right breast, with local calcifications in a clustered distribution, and an oval lump in the outer upper quadrant, with a clear border and regular edges; the subtraction image (A2, B2) shows mild enhancement of lesions. The lesions in the upper quadrant were obscure as shown in the LE image (A1, B1) but shown as moderate enhancement in the subtraction image (A2, B2). It is confirmed by pathological results as infiltrative ductal carcinoma in the outer upper quadrant and ductal carcinoma in situ in the upper quadrant.

TABLE 2. Comparing the Diagnostic Performance Between CESM and MRI

	Imaging Methods	
	CESM	MRI
Sensitivity	162/177 (91.5%)	162/177 (91.5%)
Specificity	77/86 (89.5%)	69/86 (80.2%)
Accuracy	81.0%	71.7%
Positive predictive value	162/171 (94.7%)	162/179 (90.5%)
Negative predictive value	77/92 (83.7%)	69/84 (82.1%)
False-negative rate	15/177 (8.5%)	15/177 (8.5%)
False-positive rate	9/86 (10.5%)	17/86 (19.8%)
Diagnostic conformance rate	239/263 (90.9%)	231/263 (87.8%)

Detection Results of Lesions by Imaging Examinations

The agreement between the observers for the findings was good ($\kappa = 0.820$, $P = 0.001$).

Contrast-Enhanced Spectral Mammography

A total of 259 lesions (98.5%) were detected by CESM, whereas 2 lesions of fibroadenoma, 1 lesion of breast adenosis with ductal dilation, and 1 lesion of breast adenosis with fibroma formation trend were not detected. In 259 lesions, 200 lesions were detected in both the LE images and the subtracted images, and 59 lesions were detected only in the subtracted images; 214 lesions were shown as lump-like enhancement, 31 lesions as non–lump-like enhancement, and 7 lesions as lump-like and non–lump-like enhancement. Of 59 lesions detected only in the subtraction images, 46 lesions were shown as lump-like enhancement, 9 lesions as non–lump-like enhancement, and 2 lesions as lump-like & non–lump-like enhancement; there were 18 malignant lesions and 41 benign lesions.

Magnetic Resonance Imaging

Two hundred fifty-eight lesions (98.1%) were detected by MRI. Among these, 215 lesions were shown as lump-like enhancement, 30 lesions as non–lump-like enhancement, 6 lesions as lump-like and non–lump-like enhancement, and 1 lesion as simple asymmetrical ductal dilation. In 5 lesions not detected, 3 cases were breast adenosis, 1 case was intraductal papilloma, and 1 case was ductal carcinoma in situ.

Diagnostic Efficacy of Different Imaging Examination Methods

Misdiagnosis Results of Different Examination Methods

(1) CESM: In total, 24 lesions were misdiagnosed, including 15 malignant lesions (2 lesions of BI-RADS 2, 2 lesions of BI-RADS 3, and 11 lesions of BI-RADS 4A, specifically 1 lesion of colloid carcinoma, 2 lesions of intraductal papilloma, 10 lesions of infiltrative ductal carcinoma, and 2 lesions of ductal carcinoma in situ) and 9 benign lesions (3 lesions of BI-RADS 4B and 6 lesions of BI-RADS 4C, specifically 2 lesions of breast cystic adenosis, 4 lesions of fibroadenoma, 1 lesion of sclerosing adenosis, and 2 benign lesions). In the LE images, colloid carcinoma was manifested as a high-density ellipse lump with an unclear border, accompanied by popcorn calcification, and assessed as BI-RADS 3; in the subtraction images, no enhancement was found, and it was assessed as BI-RADS 2 by CESM. In the subtraction images, ductal carcinoma in situ was manifested separately as circular mild enhancement and moderate enhancement (Fig. 3) and assessed as BI-RADS 4A; infiltrative ductal carcinoma was manifested as markedly enhanced circular nodes with a clear border and mildly enhanced irregular nodes with an unclear border and assessed as BI-RADS 4A; intraductal papilloma was manifested as irregularly mild enhancement. In all benign lesions, 1 lesion was manifested as regionally mild enhancement in the subtraction images and assessed as BI-RADS 4C; the remaining lesions were manifested as moderate and evident enhancement and assessed as BI-RADS 4B and 4C.

(2) MRI: A total of 32 lesions were misdiagnosed, including 15 malignant lesions (12 lesions of BI-RADS 4A, specifically 7 lesions of infiltrative ductal carcinoma, 2 lesions of infiltrative carcinoma with carcinoma in situ, 2 lesions of intraductal papilloma, and 1 lesion of carcinoma in situ; 1, 1, and 1 lesion of BI-RADS 1, 2, and 3, specifically 1, 1, and 1 lesion of carcinoma in situ, ductal carcinoma, and ductal carcinoma with infiltration) and 17 benign lesions (7 lesions of BI-RADS 4B, specifically 1 lesion of adenosis, 1 lesion of simple ductal dilation, and 5 lesions of fibroadenoma; 6 lesions of BI-RADS 4C, specifically 1 lesion of sclerosing adenosis, 2 lesions of adenosis, and 2 lesions of adenoma; 4 lesions of BI-RADS 5, specifically 2 lesions of adenoma, 1 lesion of cystic adenosis, and 1 benign lesion).

Diagnostic Efficacy of Each Diagnosis Methods

By evaluating the diagnostic value, the sensitivity, positive predictive value, negative predictive value, and false-negative rate from CESM examination were comparable to those from MRI (91.5%, 94.7%, 83.7%, and 8.5% vs 91.5%, 90.5%, 82.1%, and 8.5%). Importantly, the accuracy and the specificity were higher for CESM than those for MRI (81% and 89.5% vs 80.2% and 71.7%), whereas the false-positive rate was lower (10.5% vs 19.8%) (Table 2). With the pathological results as criterion standard, AUC of CESM and MRI for diagnosing benign and malignant breast lesions was 0.950 and 0.939, respectively (Table 3). There was no statistically significant difference in AUC between CESM and MRI ($Z = 0.701$, $P > 0.05$).

Correlation Between the Maximum Diameters of Lesions Measured by Different Imaging Diagnostic Methods and Pathological Results

After the rejection of cases without pathological detection records, not detected by the LE images, and of nonlump type, in total 106 cases were included into the study. We measured the maximum diameter of suspected lesions on the MR and CESM images. The mean difference between the maximum diameters of lesions measured by CESM and MRI and by pathology was −0.01 and −0.55 mm, respectively (95% confidence interval,

TABLE 3. ROC Curves of CESM and MRI on the Evaluation of Diagnostic Value

	AUC	SE	95% Confidence Interval
CESM	0.950	0.0127	0.917–0.973
MRI	0.939	0.0145	0.903–0.965

There was no statistically significant difference in AUC between CESM and MRI ($Z = 0.701$, $P > 0.05$).

TABLE 4. Comparing the Cases in the Assessing the Maximum Tumor Size Between CESM, MRI, and Histopathology

	Diameter 0.8–3 cm	Diameter 3.1–6 cm	Diameter 6.1–15 cm
CESM	78	26	2
MRI	87	16	3
Pathology	82	22	2

−0.34 to 0.31; −0.87 to −0.22 mm) (Tables 4 and 5). The correlation analysis between the results measured by MRI and the pathological results showed $r = 0.774 (P < 0.001)$, that between the results measured by CESM and the pathological results showed $r = 0.771 (P < 0.001)$, and that between the results measured by CESM and MRI results showed $r = 0.900 (P < 0.001)$ (Fig. 4).

DISCUSSION

This study demonstrated that, in 263 lesions, 259 and 258 lesions were detected by CESM and MRI, respectively; 2 examination methods display the similar sensitivity (91.5%) and false-negative rate (8.5%). It is worth mentioning that application of CESM shows higher specificity (89.5% vs 80.2%), positive predictive value (94.7% vs 90.5%), negative predictive value (83.7% vs 82.1%), and diagnostic conformance rate (90.9% vs 87.8%) than those of MRI. Although the correlation between the results measured by MRI and the pathological results was slightly stronger than that between results measured by CESM and the pathological results (0.774 vs 0.771), the difference was not statistically significant. Our results showed that CESM and MRI were comparable to the diagnostic efficacy of breast diseases and were even better than MRI in terms of specificity and diagnostic conformance rate. Moreover, in the prediction of tumor size, the difference between CESM and pathological results was not statistically significant. Therefore, we believe that CESM can well detect and diagnose breast diseases.

Magnetic resonance imaging was accepted as the best imaging method for the clinical diagnosis, staging, follow-up of breast cancer and neoadjuvant chemotherapy (NAC) response monitoring, currently. Numerous studies had proven that MRI could improve the detection sensitivity of breast cancer and greatly helps the postoperative evaluation and follow-up of breast cancer, but it had limited specificity. Its application was limited to a certain degree because MRI was expensive and time consuming and contraindicated to patients with metallic implants and pacemaker.[11,12] The cost and availability were significant barriers to widespread implementation. Contrast-enhanced spectral mammography was a new imaging technique on the basis of a combination of morphology and tumor neoangiogenesis. It displayed such advantages as simple operation, a short examination time, and low costs relative to MRI. Our study results showed that CESM was comparable to MRI in the diagnostic efficacy and even better than MRI in the specificity, accuracy, and false-positive values. On the one hand, CESM LE image can clearly show the calcification lesions in

TABLE 5. Comparing the Maximum Tumor Size on CESM Versus MRI Versus Histopathology

	Mean, cm	Mean Difference, cm	95% Confidence Interval, cm
CESM	2.63	−0.01	−0.34 to 0.31
MRI	2.43	−0.55	−0.87 to 0.22
Pathology	2.66		

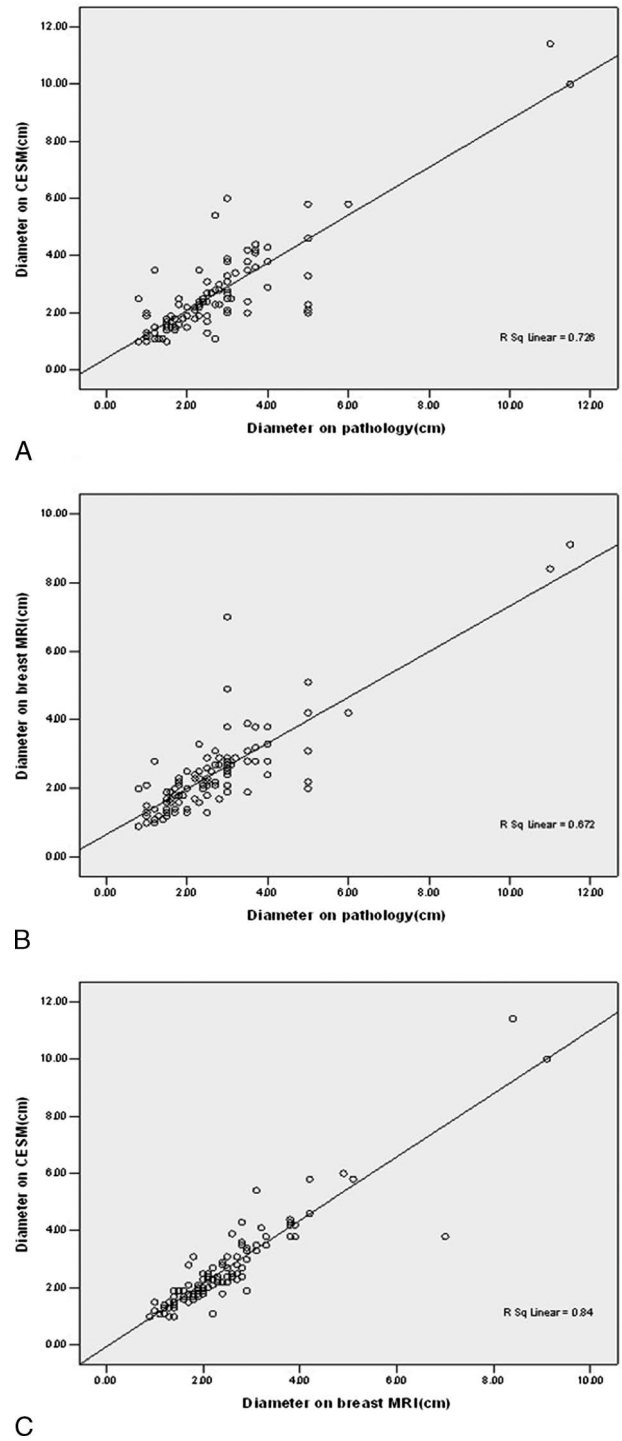

FIGURE 4. Scatterplots and Pearson correlation coefficients of maximum tumor diameter measurements among CESM and histopathology (A), MRI and histopathology (B), and CESM and MRI (C).

the breasts, especially some cluster-based, distributed, unshaped malignant calcification lesions, whereas MRI is insensitive to calcification. On the other hand, CESM is the subtraction of HE and LE images, and the lesions will not be concealed by the normal dense gland tissues in the subtraction image. Our study results are coincident to those of many reports. Jochelson et al[13] conducted a study of CESM versus MRI in 52 breast cancer patients and found that CESM and MRI had the same sensitivity, although more malignant lesions were detected by MRI, which was accompanied by more misdiagnosis. Luczynska et al[14] compared the diagnostic efficacy of MRI and CESM, and finally drew a conclusion: the sensitivity and specificity of CESM were 100% and 79%, while those of MRI were 93% and 73%; the measurement results of tumor size by CESM and MRI were similar, both slightly greater than those by pathology; as calculated, the false positive rate and false-negative rate of CESM were 20% and 0%, compared with 29% and 6% of MRI, suggesting higher diagnostic value. Some scholars believed that in diagnosing breast cancer, CESM might have slightly lower sensitivity than CE-MRI but higher specificity. In this study, the lesion sizes measured by both CESM and MRI were correlated with the pathological results, and the correlation between MRI versus pathology and CESM versus pathology were equivalence. Although the lesion size was underestimated by both examination methods, the difference was not statistically significant. This study showed that CESM subtraction images could clearly display the lesion range, which could provide great assistance for surgical management. At present, MRI is a pivotal tool to evaluate the therapeutic response for the NAC.[15] Contrast-enhanced spectral mammography has the diagnostic efficacy comparable to MRI and possesses the merits of convenient operation and low costs. Therefore, future studies are needed to investigate whether CESM can be used to evaluate the response of breast cancer to NAC.

Although CESM was similar to MR diagnosis and it had the characteristics of being less time consuming and having low cost and sensitivity to calcification, it still had shortcomings. Magnetic resonance imaging had the advantage of being able to image the entire chest wall and axilla, and it uses no ionizing radiation and does not require compression. Although iodinated contrast was generally considered to be significantly more hazardous than gadolinium contrast, whether the deposition of gadolinium had any actual consequences to human health was unknown.

CONCLUSIONS

Contrast-enhanced spectral mammography, a combination of HE image and LE image, can well display breast lesions and has the diagnostic efficacy equivalent to MRI. Importantly, CESM imaging shows higher specificity, positive predictive value, and diagnostic conformance rate than MRI. Combined with those benefits, CESM has such advantages as convenient and fast examination, strong applicability, and low costs; thus, it can be popularized as a useful tool in breast disease.

REFERENCES

1. Bhimani C, Matta D, Roth RG, et al. Contrast-enhanced spectral mammography: technique, indications, and clinical applications. *Acad Radiol*. 2017;24:84–88.
2. Patel BK, Lobbes MB, Lewin J. Contrast enhanced spectral mammography: a review. *Semin Ultrasound CT MRI*. 2018;39:70–79.
3. Mori M, Akashi-Tanaka S, Suzuki S, et al. Diagnostic accuracy of contrast-enhanced spectral mammography in comparison to conventional full-field digital mammography in a population of women with dense breasts. *Breast Cancer*. 2017;24:104–110.
4. Tagliafico AS, Bignotti B, Rossi F, et al. Diagnostic performance of contrast-enhanced spectral mammography: systematic review and meta-analysis. *Breast*. 2016;28:13–19.
5. Barra FR, de Souza FF, Camelo REFA, et al. Accuracy of contrast-enhanced spectral mammography for estimating residual tumor size after neoadjuvant chemotherapy in patients with breast cancer: a feasibility study. *Radiol Bras*. 2017;50:224–230.
6. Patel BK, Garza SA, Eversman S, et al. Assessing tumor extent on contrast-enhanced spectral mammography versus full-field digital mammography and ultrasound. *Clin Imaging*. 2017;46:78–84.
7. Lobbes MB, Lalji U, Houwers J, et al. Contrast-enhanced spectral mammography in patients referred from the breast cancer screening programme. *Eur Radiol*. 2014;24:1668–1676.
8. Evans DG, Maxwell AJ. MRI screening in women with a personal history of breast cancer. *J Natl Cancer Inst*. 2016;108:2–3.
9. Houssami N, Ciatto S, Macaskill P, et al. Accuracy and surgical impact of magnetic resonance imaging in breast cancer staging: systematic review and meta-analysis in detection of multifocal and multicentric cancer. *J Clin Oncol*. 2008;26:3248–3258.
10. Knogler T, Homolka P, Hoernig M, et al. Application of BI-RADS descriptors in contrast-enhanced dual-energy mammography: comparison with MRI. *Breast Care*. 2017;12:212–216.
11. Tudorica A, Oh KY, Chui SY, et al. Early prediction and evaluation of breast cancer response to neoadjuvant chemotherapy using quantitative DCE-MRI. *Transl Oncol*. 2016;9:8–17.
12. Roganovic D, Djilas D, Vujnovic S, et al. Breast MRI, digital mammography and breast tomosynthesis: comparison of three methods for early detection of breast cancer. *Bosn J Basic Med Sci*. 2015;15:64–68.
13. Jochelson MS, Dershaw DD, Sung JS, et al. Bilateral contrast-enhanced dual-energy digital mammography: feasibility and comparison with conventional digital mammography and MR imaging in women with known breast carcinoma. *Radiology*. 2013;266:743–751.
14. Jakubowicz J, Heinze-Paluchowska S, Hendrick E, et al. Comparison between breast MRI and contrast-enhanced spectral mammography. *Med Sci Monit*. 2015;21:1358–1367.
15. Marinovich ML, Macaskill P, Irwig L, et al. Agreement between MRI and pathologic breast tumor size after neoadjuvant chemotherapy, and comparison with alternative tests: individual patient data meta-analysis. *BMC Cancer*. 2015;15:1–12.